Potential effects of deep seawater discharge by an Ocean Thermal Energy Conversion plant on the marine microorganisms in oligotrophic waters

Mélanie Giraud, Véronique Garçon, Denis de La Broise, Joël Sudre, Stéphane L'Helguen, Marie Boye

Potential effects of deep seawater discharge by an Ocean Thermal Energy Conversion plant on the marine microorganisms in oligotrophic waters

Mélanie Giraud[1,2,3], Véronique Garçon[2], Denis de la Broise[1], Stéphane L'Helguen[1], Joël Sudre[2], Marie Boye[1,4]

[1]LEMAR (UMR 6539), IUEM, Technopôle Brest-Iroise, 29280 Plouzané - France ; [2]LEGOS (UMR 5566), 31401 Toulouse cedex 9 - France ; [3]France Energies Marines, 29200 Brest - France ; [4]Present address : Institut de Physique du Globe de Paris (UMR 7154), 75005 Paris, France

Corresponding author: M. Boye (boye@ipgp.fr)

Science of the Total Environment 693 (2019) 133491
https://doi.org/10.1016/j.scitotenv.2019.07.297

Abstract

Installation of an Ocean Thermal Energy Conversion pilot plant (OTEC) off the Caribbean coast of Martinique is expected to use approximately 100 000 m^3 h^{-1} of deep seawater for its functioning. This study examined the potential effects of the cold nutrient-rich deep seawater discharge on the phytoplankton community living in the surface warm oligotrophic waters before the installation of the pilot plant. Numerical simulations of deep seawater upwelled by the OTEC, showed that a 3.0 °C temperature change, considered as a critical threshold for temperature impact, was never reached during an annual cycle on the top 150 m of the water column on two considered sections centered on the OTEC. The thermal effect should be limited, less than 1 km^2 on the area exhibited a temperature difference of 0.3 °C (absolute value), producing a negligible thermic impact on the phytoplankton assemblage. The impact on phytoplankton of the resulting mixed deep and surface seawater was evaluated by *in situ* microcosm experiments. Two scenarios of water mix ratio (2 % and 10 % of deep water) were tested at two incubation depths (deep chlorophyll-*a* maximum: DCM and bottom of the euphotic layer: BEL). The larger impact was obtained at DCM for the highest deep seawater addition (10 %), with a development of diatoms and haptophytes, whereas 2 % addition induced only a limited change of the phytoplankton community (relatively higher *Prochlorococcus sp.* abundance, but without significant shift of the assemblage). This study suggested that the OTEC plant would significantly modify the phytoplankton assemblage with a shift from pico-phytoplankton toward micro-phytoplankton only in the case of a discharge

affecting the DCM and would be restricted to a local scale. Since the lower impact on the phytoplankton assemblage was obtained at BEL, this depth can be recommended for the discharge of the deep seawater to exploit the OTEC plant.

Keywords: marine microbial ecosystem | biogeochemistry | modeling | artificial seawater discharge | *in situ* experiments | environmental standards

1. Introduction

Ocean Thermal Energy Conversion (OTEC) uses the solar energy by exploiting the temperature gradient between surface and bottom seawater. In an OTEC plant, the cold deep seawater pumped close to sea bottom is used to condense a working fluid (like ammonia), whereas warm surface waters, pumped close to the surface, serve to evaporate it. The difference of pressure, generated by the evaporation and condensation of the fluid, drives a turbine that produces mechanical energy. This energy is then converted to electrical energy in a generator. Due to the need of a 20 °C difference between the cold deep and the warm surface waters for the OTEC exploitation, tropical areas are well suited for the installation of OTEC plants.

The Martinique, a tropical island of Lesser Antilles, is ideally suited for OTEC functioning with its narrow continental slope in the Caribbean part of the island, allowing an implementation of the plant close to the coast. The implementation of a 10 MW OTEC pilot plant off the Caribbean coast of Martinique is expected in 2020 as part of the french NEMO project (Akuo Energy, DCNS). This OTEC will pump approximately 100 000 $m^3.h^{-1}$ of deep seawater at 1100 m depth. In order to optimize the energy efficiency, the deep seawater should be rejected close to the surface. However, this large discharge could induce important disturbances on the upper ocean ecosystem, and this impact should be estimated.

Environmental assessment of OTEC functioning was studied since the 1980's (NOAA, 1981; 2010). The deep seawater discharge was described as one of the major drivers impacting the marine environment in OTEC plant. However, only a few studies specifically detailed this critical aspect (Taguchi et al., 1987; Rocheleau et al., 2012). The deep seawater discharge in OTEC plant generates a phenomenon similar to the one naturally occurring in the ocean within upwelling systems. Equatorward winds along the coast in the eastern Atlantic and Pacific linked to atmospheric high-pressure systems force Ekman transport and pumping, relocating coastal

surface waters offshore. Thereby, deep water transport towards the surface is generated close to the coast. In these systems, the large amount of macronutrients and trace metals carried to the euphotic zone by the enriched deep seawater supports a large development of the phytoplankton, making upwelling the most productive oceanic regions (Bakun, 1990; Pauly and Christensen, 1995; Chavez and Toggweiler, 1995; Carr and Kearns, 2003). By contrast, the tropical surface waters off the Caribbean coast of Martinique exhibit low nutrients (nitrate and phosphate) concentrations (< 0.02 $\mu mol.L^{-1}$) and therefore, they can be significantly enriched by the deep seawater discharge. Whereas phytoplankton assemblages in upwelling systems are usually dominated by large phytoplankton and particularly by diatoms (Bruland et al., 2001; Van Oostende et al., 2015), the phytoplankton community in oligotrophic systems is composed of smaller organisms (Agawin et al., 2000).

Due to these important differences in biogeochemical functioning and environmental microbiology, it is thus of critical interest to investigate the potential effects of the deep seawater discharge of the planned OTEC plant on the phytoplankton community off Martinique. Furthermore, it is crucial to provide a depth where the deep seawater could be discharged without significant effect on the surface layer where phytoplankton is the most abundant. Indeed, no environmental standards on the deep seawater discharge effects are available yet, while transitional blue energies such as OTEC plants will likely expand in the near future.

In this study, the impact of deep seawater discharge on the thermal structure of surface waters was first assessed. Modification of the surface waters stratification should indeed impact the phytoplankton community. A high-resolution oceanic model was used to examine the thermal impact induced by the deep seawater dispersion. Eight configurations of discharge depth were tested, corresponding to the deep chlorophyll-*a* maximum (DCM), the bottom of the euphotic layer (BEL) and five depths below the BEL. Temperature differences between numerical simulations without and with the deep seawater discharge were compared on the upper 150 m of a vertical section.

The distribution of the ambient phytoplankton community and the biogeochemical properties of the deep and surface seawater mixture that could impact the phytoplankton community were then described. Phytoplankton distribution and assemblage were detailed in order to assess short time and small scales variabilities of phytoplankton assemblage and primary production in the study site.

85 Finally, in order to simulate the OTEC deep seawater input, enrichment experiments were conducted on
86 the future site of the pilot plant. Enrichment experiments are commonly used in oceanography to assess the
87 effects on phytoplankton community and primary production. For example, large iron (Fe) enrichment
88 experiments were conducted from 1993 to 2005 to estimate the potential of Fe limitation on ocean primary
89 production (De Baar et al., 2005; Boyd et al., 2007). Several experiments also showed that macro- and micro-
90 nutrients enrichments induce changes in the phytoplankton community in upwelling regions (Hutchins et al.,
91 2002) as well as in oligotrophic regions (Kress et al., 2005). Enrichment experiments were usually conducted with
92 mesocosms immerged close to the surface (Escaravage et al., 1996; Duarte et al., 2000) or in laboratory under
93 artificial light and temperature using phytoplankton model species (Brzezinski, 1985). A laboratory experiment
94 intended to evaluate the effects of an OTEC seawater discharge in Hawaiian waters on the natural
95 phytoplankton community was previously conducted (Taguchi et al., 1987) under such artificial conditions, and
96 thus, it could not totally reproduce what occurred in the natural environment. Other deep seawater discharge
97 experiments were realized *in situ* (Aure et al., 2007; Handå et al., 2014). For example, the use of a moored
98 platform to upwell deep seawater and discharge it close to the surface has shown an increase in primary
99 production in a western Norwegian fjord where the euphotic zone is nutrient-depleted during summer (Aure et
100 al., 2007), as it would be expected with the OTEC discharge in oligotrophic waters. Whereas such a pumping
101 system is well adapted for pumping seawater at 30 m depth for example, it cannot be applied for OTEC
102 experiments where deep seawater must be collected far deeper (1100 m depth) and also discharged more
103 deeply in the water column to reduce the potential effects on the phytoplankton community. These conditions
104 can be obtained by the use of *in situ* microcosms, in which light and temperature are the same as in the natural
105 surrounding waters, avoiding additional bias, and several conditions (enrichment, incubation depth) can be
106 simulated. Therefore, we used the unique device of immerged microcosms we developed (Giraud et al., 2016)
107 for assessing the effects of deep seawater discharge on the phytoplankton community. Two incubation depths
108 (DCM and BEL) with two ratios of enriched seawater (mixtures of surface water with 2 % and 10 % of deep
109 seawater) were tested.
110 These experiments allowed the evaluation of critical mixing rate and discharging depth where effect was
111 maximal.

112 **2. Materials and methods**

2.1. Modelling the thermal effect

The hydrodynamic numerical model ROMS-Regional Ocean Model System (Shchepetkin and McWilliams, 2005; 2009) was used to describe the resulting thermal effect due to OTEC functioning. The model was run in a 2-ways AGRIF configuration allowing to define a parent and child domains around the Martinique Island which are run simultaneously, transferring automatically open boundary conditions. The parent grid ranges from 63° W to 59° W and 13° N to 15.9° N with a resolution of 1/60° (around 1.8 km) while the child domain narrows the parent one and was from 61.74° W to 60.41° W and 14.21° N to 15.11° N with a resolution down to 1/180° (around 600 m). The bottom topography and coastline are interpolated from the GINA database (1/120°, www.gina.alaska.edu/data/gtopo-dem-bathymetry) (Fig. 1). The model is forced by the monthly Climate Forecast System Reanalysis (NCEP-CFSR) for wind stress, heat and freshwater fluxes. For the open boundary conditions and initial conditions of the parent domain, a monthly climatology computed from the Simple Ocean Data Assimilation (SODA) reanalysis (Carton and Giese, 2008) was used for the dynamical variables (temperature, salinity and velocity fields). The configurations were run without and with a deep seawater discharge mimicking the OTEC functioning (Giraud, 2016). Eight cases of horizontal discharge settings were simulated at different depths: i) the DCM (45 m), ii) the BEL (80 m), that were estimated on June 12th 2014, and 3) six depths below the euphotic zone (110 m, 140 m, 170 m, 250 m, 350 m and 500 m). In the OTEC plant, deep water will be pumped at 1100 m where temperature is around 5 °C and salinity 35. Circulation of this water through the plant system will warm it up until 8 °C prior to its release in the upper ocean. We thus applied at the location of the OTEC plant (61°13'0'' W, 14°35'48'' N), a cold-water discharge (temperature 8 °C, salinity 35) at a flow rate of 28 m^3 s^{-1} and with a northward orientation. The thermal impact of the cold-water source was assessed documenting the differences between simulations without and with the modelled OTEC plant functioning (Giraud, 2016).

2.2. Field observations and *in situ* experiments

2.2.1. Sampling and analytical methods

Temperature, salinity, and fluorescence profiles were performed on 12th, 13th, 18th and 19th of June 2014 using Seabird SBE19+ probe with *in situ* Fluorimeter Chelsea AQUAtracka III.

139 Seawater was collected on 12th and 18th of June 2014 in the water column in ultra-clean conditions (Giraud
140 et al., 2016) to measure *in situ* parameters and to prepare the microcosms. Seawater and microcosms were
141 sampled similarly in a land laboratory a few hours after collection.

142 Nitrate (NO_3^-), nitrite (NO_2^-), phosphate (PO_4^{3-}) and silicate ($Si(OH)_4$) concentrations were determined in
143 filtered waters (<0.6 µm; PC membrane) stored at -20 °C until analysis using a Bran + Luebbe AAIII auto-
144 analyzer (Aminot and Kérouel, 2007).

145 Filtered samples (0.2 µm; 300AC-Sartobran™ capsules) for dissolved trace metals determination were
146 collected under pure-N_2 pressure (0.7 atm) in acid cleaned low density polyethylene bottles, acidified with
147 ultrapure HCl (pH < 2) and stored in two plastic bags in dark at ambient temperature. Concentrations of
148 dissolved trace metals (cadmium: Cd; lead: Pb; iron: Fe; zinc: Zn; manganese: Mn; cobalt: Co; nickel: Ni; and
149 copper: Cu) were determined in UV-digested samples by ID-ICP-MS (Milne et al., 2010) after preconcentration
150 on a WAKO resin (Kagaya et al., 2009) using an Element XR ICP-MS. Blanks, limits of detection, accuracy and
151 precision (assessed using reference samples) of the ID-ICP-MS method are reported in Table 1. The values
152 determined by ID-ICP-MS were in excellent agreement with the consensus values, apart for Cd that yielded
153 higher concentration in S-SAFE reference sample than the consensus value (Table 1).

154 The pH was determined using a pH ultra-electrode (pHC28) mounted on a HQ40d multi pH-meter (HACH)
155 with an accuracy of ± 0.002 pH unit in samples preserved with saturated $HgCl_2$ in glass bottles hermetically
156 closed with Apiezon grease, sealed with Parafilm® and stored in the dark at ambient temperature.

157 Three complementary methods were used to analyze the phytoplankton community. Pigment signatures
158 were measured by HPLC (using an Agilent Technologies 1100-series) on polysulfone filters (0.22 µm pore-size)
159 frozen at -20 °C and stored in liquid nitrogen, after internal standard addition (vitamin E acetate) and extraction
160 in a 100 % methanol solution (Hooker et al., 2012). Fifty pigments were identified and associated to
161 phytoplankton groups (Uitz et al., 2010). Identification and enumeration of pico-phytoplankton were realized by
162 flow-cytometry using a BD-FACSVerse™ (Marie et al.,1999) in samples preserved in cryotube with addition of
163 0.25 % glutaraldehyde frozen at -20 °C and stored in liquid nitrogen. Four groups of pico-phytoplankton were
164 identified: *Prochlorococcus*, picoeukaryotes (< 10 µm), and 2 groups of *Synechococcus* discriminated,
165 respectively, by their low and high phycourobilin (PUB) to phycoerythrobilin (PEB) ratios. Taxonomic
166 identification and enumeration of micro-phytoplankton (20-200 µm) and a part of nano-phytoplankton (2-20 µm)

(Dussart, 1966) were carried out using an inverted microscope (Wild M40) in samples preserved with neutral lugol solution. Utermöhl settling chambers (Hasle, 1988) were used for micro-phytoplankton analyses, and a smaller sedimentation chamber (2.97 mL) for the analyses of nano-phytoplankton. When possible, phytoplankton was identified to the lowest possible taxonomic level (species, genus or group) using the classical manual for marine phytoplankton identification (Thomas, 1996) and the World Register of Marine Species database (WoRMS Editorial Board, 2019). Biovolume of each species was also estimated from these microscope analyses (Hillebrand et al., 1999).

2.2.2. *In situ* microcosm experiments

The potential impact of deep seawater discharge on the phytoplankton community was simulated by *in situ* microcosm incubations of various deep and surface seawater mixing (Giraud et al., 2016). The experiments were conducted from 12th (D0) to 19th (D7) of June 2014. The deep and surface seawaters were collected at the site of the future OTEC pilot plant (61°11'52'' W-14°37'57'' N; Fig. 1). Microcosms bottles were incubated on two stainless steel structures set at the depths of deep chlorophyll-*a* maximum (DCM) and at the bottom of the euphotic layer (BEL) on a mooring chain located, for practical reasons, closer to the coast (61°10'9'' W-14°39'8'' N, seafloor at 220 m depth) during 6 days (Giraud et al., 2016). This incubation time was chosen to represent the short-term phytoplankton response time to a mixing of deep water with surface waters. This duration is shorter or equal than the residence time of the enriched water mass, which is less than one month.

Seawater was collected at D0 at the depths of DCM (45 m depth) and BEL (80 m depth) identified on the future OTEC site from the fluorescence profile, and close to the bottom (1100 m depth corresponding to the pumping depth of the future OTEC plant) in ultra-clean conditions. Deep seawater was mixed in three proportions (0 % as a control hereafter referred to as "Control", 2 % as a low input called "2 % of deep seawater", and 10 % as a large input called "10 % of deep seawater") with DCM and BEL waters. Each resulting mixture was distributed in 2.3 L polycarbonate bottles filled up to overflow level, of which four replicates per mixing condition per depth were immersed at their respective sampling-depth for 6 days; duplicates per mixing condition per depth were kept in dark at 25 °C for a few hours until sampling for later characterization of phytoplankton assemblage and biogeochemical properties at D0 (called "Surrounding waters D0"); and

duplicates per mixing condition per depth were used to estimate carbon and NO_3^- uptakes at D0 (called "Surrounding waters D0") as described below.

Same sampling and mixtures were realized at day 6 (D6, June 18th) just to evaluate the temporal evolution in the natural environment, resting on duplicate bottles per mixing condition per depth for phytoplankton and biogeochemical characterizations at D6 (called "Surrounding waters D6") and using other duplicates to estimate carbon and NO_3^-uptakes at D6 (called "Surrounding waters D6").

After the 6 days incubation, all the incubated microcosm bottles on the mooring (called "Microcosm D6") were brought on board. A quarter of each four replicates per condition was put in a new 2.3 L clean bottle and used to estimate carbon and NO_3^- uptakes after 6 days of incubation (called "Microcosm D6"). The remaining microcosm contents were kept for sampling and analysis.

2.2.3. Carbon and nitrate uptakes

Carbon (primary production) and NO_3^- uptake rates were estimated in the same sample using the dual $^{13}C/^{15}N$ isotopic label technique (Slawyk et al., 1977). Immediately after sampling, ^{13}C tracer ($NaH^{13}CO_3$, 99 atom%, Eurisotop, 0.25 $mmol^{13}C.mL^{-1}$) and ^{15}N tracer ($Na^{15}NO_3$, 99 atom%, Eurisotop, 1 $\mu mol^{15}N.mL^{-1}$) were added to seawater mixtures at 10^{-3}:1 v/v ratio. The initial enrichment was 10 atom% excess of ^{13}C for the bicarbonate pool and 16-95 atom% excess of ^{15}N for the NO_3^- pool depending on the ambient NO_3^- concentration. The $^{13}C/^{15}N$ amended bottles were incubated for 24 h on the mooring line at the DCM and BEL depths, after which 1 L samples were filtered onto pre-combusted (450 °C, 4 h) glass fiber filters (Whatman). Filters were stored at -20 °C and oven dried (60 °C, 24 h) prior to analysis. Concentrations of carbon (POC), nitrogen (PON) as well as ^{13}C and ^{15}N enrichments in particulate matter were measured with a mass spectrometer (Delta plus, ThermoFisher Scientific) coupled to a C/N analyzer (Flash EA, ThermoFisher Scientific). Standard deviations were 0.009 µM and 0.004 µM for POC and PON, and 0.0002 atom% and 0.0001 atom% for ^{13}C- and ^{15}N-enrichments, respectively.

The absolute uptake rates (ρ, in $\mu mol.L^{-1}.h^{-1}$) were calculated for nitrogen (Dugdale and Wilkerson, 1986) and carbon (Fernández et al., 2005) using the particulate organic concentrations measured after 24 h of incubation. These rates were converted into biomass specific uptake rates (V_C or V_{NO3^-}, in $\mu mol.(\mu g\ Chl\ a)^{-1}.h^{-1}$) by dividing ρ by the total chlorophyll *a* concentration (TChl *a* defined as the sum of chlorophyll *a* and divinyl chlorophyll *a*) measured at the end of the incubations. The addition of ^{15}N tracer would cause a substantial

222 increase in dissolved inorganic nitrogen concentrations especially in the surface waters and, in turn, an
223 overestimation of uptake rates (Dugdale and Wilkerson, 1986; Harrison et al., 1996). The NO_3^- uptake rates
224 were corrected for this perturbation (Dugdale and Wilkerson, 1986) using a half-saturation constant of 0.05
225 $\mu mol.L^{-1}$ characteristic for nitrogen-poor oceanic waters (Harrison et al., 1996) and the measured NO_3^-
226 concentration. Overestimation was low (< 5 %) in samples with an addition of deep seawater but it was of about
227 50 % in samples without deep seawater addition. The uptake rates measured in these samples represented
228 therefore estimations rather than actual values.

229 #### 2.2.4. Statistical analyses

230 Kruskal-Wallis test was applied on the set of pigments concentrations, pico-phytoplankton abundances
231 and macronutrients concentrations. If significant differences ($p < 0.05$) were found, Mann-Whitney test was run
232 to identify the samples significantly different. Statistical analyses were performed using Statgraphics Centurion
233 XVI software.

234 ## 3. Results

235 ### 3.1. Impact of the deep seawater discharge on the thermal and density structure in surface

236 The representation of the thermocline and halocline depths, key proxies for oceanic mixing and for
237 estimating the thermal impact of the OTEC discharge, is well mimicked over the 2 months (June and
238 November) of the mesoscosm experiments (Giraud, 2016). In order to assess the deep seawater discharge
239 impact on the thermal structure of the upper 150 m of the water column, the dispersion of temperature
240 differences (ΔT in °C) obtained without and with the deep seawater discharge in the model outputs was
241 examined on two vertical sections. A section of 124 km for the large domain (corresponding to the child
242 domain) and another section of 10 km for the near-OTEC domain (defined from 61.24° W to 61.17° W and
243 14.60° N to 14.67° N) were defined, both centered on the OTEC site and parallel to the coast (Fig. 1).

244 Presently, there are no environmental standards defining threshold levels for temperature difference that
245 will be induced by an OTEC deep seawater discharge. So, the study relied on the World Bank Group
246 prescriptions for liquefied natural gas facilities which set at 3 °C the temperature difference limit at the edges of
247 the zone where initial mixing and dilution take place (IFC, 2007). We thus considered for each discharge depth
248 the cooling and warming outputs from the model, which exhibit a $|\Delta T| \geq 3$ °C. Areas (in % of the considered
249 domain) impacted by these cooling and warming effects were added (absolute values) in order to compare the

potential impact of each discharge depth configuration. None of the discharge depth configurations could produce a modification of the thermal structure of the top 150 m of the water column, higher than or equal to the considered temperature threshold ($|\Delta T| \geq 3$ °C), for both domain sections.

Then, a lower temperature difference of 0.3 °C (absolute value) was considered. This temperature difference represented a low threshold as compared to the World Bank Group prescriptions (IFC, 2007) that instead represent a high threshold. The areas exhibiting a $|\Delta T| \geq 0.3$ °C in the top 150 m (Table 2) were extremely small (< 1 km^2) and were not significantly different in both sections and at the different discharge depths, on an annual average and in June (our experimental period).

We also investigated the OTEC impact on density. The density of water being discharged at 45 m, depth of the deep chlorophyll maximum (DCM), is 27.48 (8°C and salinity of 35). The density of water at 45 m is around 23.72 (temperature of 28°C and salinity of 36.5) so the nominal density gradient is of 3.76. If one considers a modification of the density structure of the top 150 m of the water column of $|\Delta\rho| \geq 0.1$, there is no impact when the discharge occurs at the depth of the DCM. If one considers a lower density difference of 0.05 (absolute value), the area exhibiting a $|\Delta\rho| \geq 0.05$ in the top 150 m is extremely small (< 1.5 km^2) in both sections at the depth of the chlorophyll maximum. As far as we know, there are no environmental standards defining threshold levels for density difference that will be induced by an OTEC deep seawater discharge. This represents less than 1.5 % of the nominal density gradient so as for the thermal impact, the impact is estimated to be minor.

3.2. Biogeochemical properties and phytoplankton community

3.2.1. Expected biogeochemical properties of the resulting mixed waters

The pH was very similar at the DCM and BEL at the OTEC site on D6 (8.24 and 8.25, respectively), whereas deep seawater-pH showed lower value (7.81). The addition of 2 % and 10 % deep seawater to surface waters could thus induce a pH-decrease of respectively, 0.01 and 0.07 unit. Hence, the effect on pH could be rather limited compared to the 0.1 pH decrease (from 8.2 to 8.1) between the pre-industrial time and the 1990's (Orr et al., 2005).

NO_3^- and PO_4^{3-} concentrations (Table 3) were below the detection limit (< 0.02 µM) at the DCM (55 m) and BEL (80 m) at the OTEC site on observational D4 (June 16th 2014), whereas $Si(OH)_4$ concentrations were above detection limit (> 0.08 µM), particularly at the DCM (2.4 µM). NO_2^- concentrations showed the highest values at

278 the BEL whereas they were negligible at the DCM (<0.02 µM). In deep seawater, as commonly observed, NO_3^-,
279 PO_4^{3-} and $Si(OH)_4$ concentrations were largely higher compared to the surface (Table 3). The 2 % and 10 % deep
280 water additions represented a large input for NO_3^- in surface waters (from <0.02 µM to 0.54 and 2.71 µM,
281 respectively; Table 3). If the 10 % ratio also induced a large input of PO_4^{3-} (from <0.02 to 0.19 µM), the input of
282 2 % deep water was more limited (0.04 µM). The effect of 2 % or 10 % deep seawater addition was more
283 limited for $Si(OH)_4$ relatively to NO_3^- and PO_4^{3-} input, yet it accounted for 50-63 % increase for 10 % deep
284 seawater addition (Table 3). Finally, because deep and DCM waters were NO_2^- depleted, the deep seawater
285 input did not modify the NO_2^- concentration at the DCM. At the BEL, NO_2^- concentration was higher and the 10
286 % addition slightly diluted NO_2^- at this depth.

287 Mn showed maximum concentrations in the surface layer on D4 at the OTEC site (Table 4) decreasing with
288 depth as observed close to the Lesser Antilles in the Atlantic Ocean (Mawji et al., 2015), but the measured
289 surface concentrations were particularly high, especially at the DCM. Fe that commonly dispatches hybrid
290 distribution combining a nutrient-type profile in surface waters and a scavenged-type distribution in deep
291 waters (Bruland, 2003) also exhibited high surface values, particularly at the DCM (Table 4). Cd, Zn, Co, Ni, and
292 Cu dispatched nutrient-type profiles, whereas Pb exhibited scavenged-type profile (Nozaki, 1997; Gruber,
293 2008), but like for dissolved Fe and Mn, their concentrations in the upper waters were particularly high (Table
294 4). For all trace metals at both depths, the 2 % deep seawater addition will not induce significant changes in
295 their surface concentrations (Table 4). The 10 % deep seawater addition could increase Cd, Ni and Zn
296 concentrations in surface waters (Table 4), whereas it would not constitute an input of Pb, Cu, Co, and Fe, and it
297 can even dilute Mn (Table 4).

298 The surface waters can thus be enriched in macronutrients (NO_3^-, PO_4^{3-}) when submitted to a deep
299 seawater discharge (particularly with 10 % deep seawater addition) in proportion depending on the depth. The
300 same scheme can be applied in some of the dissolved trace metals (Cd, Ni, Zn) when a large ratio of deep
301 seawater (10 %) is discharged.

302 ### 3.2.2. Phytoplankton community in the natural environment

303 A set of seven accessory pigments identified as biomarkers of specific taxa (Uitz et al., 2010; Table 5) were
304 analyzed at OTEC station at D0, D4 and D6 in surrounding surface waters (Fig. 2), as well as population
305 abundance and their biovolume using light microscopy (Fig. 3).

306 TChl *a*, a proxy of the phytoplankton biomass, was higher at DCM than at BEL, as usually observed, by
307 about two-folds. The fucoxanthin (biomarker of diatoms) concentrations were similar at the DCM and BEL on D0
308 (Fig. 2), like the total abundance of diatoms (Fig. 3). Fucoxanthin concentration increased by D4 and then by D6
309 at the DCM, corresponding to increases of cumulated diatoms biovolume on D4 (Fig. 3) and of diatoms
310 abundance on D6 (Fig. 3). Peridinin, a biomarker of dinoflagellates, was detected at the DCM unlike at the BEL,
311 with relatively high abundance and biovolume of dinoflagellates (Fig. 3). The 19'-hexanoyloxyfucoxanthin
312 (biomarker of haptophytes) concentration (Fig. 2) and the prymnesiophytes (haptophyte) abundance and
313 biovolume (Fig. 3) showed higher values at the DCM than at the BEL only at D4.

314 At the DCM, dinoflagellates largely dominated the nano- and micro-phytoplankton assemblage with the
315 largest abundance and biovolume. Whereas prymnesiophytes showed the second highest abundance, its
316 biovolume was very low, on the contrary to diatoms that dispatched lower abundance but higher biovolume
317 (Fig. 3). At the BEL, dinoflagellates, prymnesiophytes and diatoms showed similar abundance, dinoflagellates
318 and the diatoms occupied the major part of the total biovolume. Three groups of dinoflagellates were observed
319 by light microscopy but they could not be identified at species level. However, their small size and the lack of
320 colored starch (using lugol) in the cytoplasm suggested they were mixotrophic or heterotrophic population.
321 Furthermore, the low concentrations of peridinin in samples supported this assumption.

322 At both depths, light microscopy analyses suggested that the large cyanobacteria, mainly
323 *Trichodesmium sp.*, were low in abundance and biovolume. Flow cytometry identification and count
324 indicated that the small cyanobacteria *Prochlorococcus* dominated the pico-phytoplankton assemblage,
325 but they showed a significant decrease from D0 to D6 (Fig. 4). A significant portion of *Synechococcus*
326 was also observed while picoeukaryotes were poorly represented. Both *Prochlorococcus* and
327 *Synechococcus* showed higher abundance at the DCM than at the BEL (by 65 % and 86 %,
328 respectively), in line with the pigment analyses of zeaxanthin (biomarker of cyanobacteria) and total
329 chlorophyll *b* concentrations (prochlorophytes).

330 **3.2.3. Primary production and nitrate uptake in the natural environment**

331 The phytoplankton distribution and assemblage can partly drive the intensity of primary production, so the
332 specific uptake rate of carbon (V_C; Fig. 5) and NO_3^- (V_{NO3-}) were estimated at D0 and D6.

333 V_C in surrounding surface waters was relatively low at D0 (Fig. 5) indicating low primary production in these
334 poor-nutrients waters. Yet, V_C was approximately three-times higher at the DCM (0.058 µmol C.(µg Chl *a*)$^{-1}$.h^{-1})
335 than at the BEL (0.017 µmol C.(µg Chl *a*)$^{-1}$.h^{-1}) at D0, but drastically decreasing on D6 at the DCM (to ~0.014
336 µmol C.(µg Chl *a*)$^{-1}$.h^{-1}). V_{NO3^-} were also very low at D0 (0.014 µmol N.(µg Chl *a*)$^{-1}$.h^{-1} at DCM, 0.017 µmol N.(µg
337 Chl *a*)$^{-1}$.h^{-1} at BEL) and drastically decreased at D6, below the detection limit (data not shown).

338 **3.3. Impacts on the phytoplankton community of the deep seawater discharge**

339 **3.3.1. Changes in the phytoplankton assemblage**

340 At the DCM, TChl *a* was similar in all treatments ($p < 0.05$) after 6 days of incubation in microcosms (Fig.
341 6). Only fucoxanthin and 19'-butanoyloxyfucoxanthin showed significant ($p < 0.05$) higher concentrations in 10
342 % enrichments as compared to controls, indicating higher abundance and/or biovolume of diatoms and
343 haptophytes. The other diagnostic pigments did not show any significant difference between enriched
344 microcosms and controls. Picoeukaryotes and *Synechococcus* abundances did not show significant variations
345 between the treatments (Fig. 7a). Reversely, *Prochlorococcus* population showed higher ($p < 0.05$) abundance
346 both in 2 % and 10 % enriched microcosms as compared to controls (Fig. 7a).

347 At the BEL, after the 6 days incubation period, pigments concentrations were below the detection limit
348 indicating very low abundance of phytoplankton. Pico-phytoplankton did not show significant variations
349 between the treatments and the controls (Fig. 7b). Pico-phytoplankton were clearly much less abundant at the
350 BEL (< 1000 cells.mL^{-1}) than at DCM (Fig. 7b), 20-times even lower than that observed in surrounding waters at
351 this depth on D6. For comparison, total abundance at the DCM was ~5-times lower in incubated microcosms on
352 D6 compared to surrounding surface waters.

353 **3.3.2. Changes in the primary production and nitrate uptake**

354 Deep water inputs (2 % and 10 %) to surrounding waters collected at the DCM on D0 led to an increase of
355 V_C within 24 h compared to the controls (by 42 % and 49 %, respectively; Fig. 5); but they had no effect on D6
356 despite very low value in natural waters at this depth (0.014 µmol N.(µg Chl *a*)$^{-1}$.h^{-1}). The 6 days incubated
357 microcosms showed very low V_C in all treatments (Fig.5). At the BEL, V_C were quite similar on D0 and D6 and
358 after 6 days of incubation. Vc increased by 57% with 10% addition of deep water on Do and was approximately
359 two times higher than the control with the two enrichments on D6 (Fig. 5). V_{NO3^-} measured in microcosms after a
360 6-days *in situ* incubation were below the detection limit (data not shown).

4. Discussion

4.1. Natural variabilities in the oligotrophic area

4.1.1. Biogeochemistry and phytoplankton community structure

The very low PO_4^{3-} and NO_3^- concentrations recorded in the oligotrophic surrounding surface waters were likely favorable to the development of small phytoplankton, especially to the cyanobacteria as shown with the significant occurrence of *Prochlorococcus* in these waters, which are typical of poor nutrient waters (Partensky et al., 1999). In line with the very low V_{NO3^-} measured here, it has been shown that V_{NO3^-} by *Prochlorococcus* represents indeed only 5-10 % of its nitrogen uptake whereas reduced nitrogen substrates (NO_2^-, ammonium, and urea) uptake accounts for more than 90-95 % (Casey et al., 2007). By contrast, the development of larger phytoplankton taxa (particularly diatoms), which have higher NO_3^- and PO_4^{3-}requirements for their growth, were probably limited by these elements. Actually, NO_3^- and PO_4^{3-} concentrations in surrounding waters at the DCM were both lower than the detection limit (< 0.02 µM at D4) which is much lower than the average values of half-saturation constants for diatoms (1.6 ± 1.9 µM for NO_3^- and 0.24 ± 0.29 µM for PO_4^{3-}; Sarthou et al., 2005). For $Si(OH)_4$, surrounding surface concentrations at DCM (2.39 µM) were in the range of diatoms half-saturation constants (3.9 ± 5.0 µM; Sarthou et al., 2005), hence the diatoms development was probably not limited by $Si(OH)_4$. Furthermore, diatoms showed low abundance in spite of relatively high $Si(OH)_4$ and dissolved trace metals (in particular Fe) concentrations in surface waters. The potential of Fe limitation on phytoplankton community has been reported previously in upwelling systems, with an apparent half-saturation constant for diatoms growth of 0.26 nM Fe in the Peru Upwelling system (Hutchins et al., 2002). This constant is far lower than the concentration of Fe measured in surrounding waters at DCM (1.08 ± 0.03 µM at D4), suggesting that diatoms were probably not limited by Fe. This further supports growth limitation of diatoms by NO_3^- and/or PO_4^{3-}.

Advection of waters from Amazon and Orinoco rivers can explain the relatively high $Si(OH)_4$ observed in the Caribbean Sea. However, little information is available on the input of trace metals by these waters into the Caribbean Sea. Amazon river can be a source of dissolved Fe, Cu, Ni, Pb and Co for the western-subtropical North Atlantic (Tovar-Sanchez and Sañudo-Wilhelmy, 2011), but this input can decrease rapidly away from its source like it has been shown for Co in the Western Atlantic (Dulaquais et al., 2014). Those inputs into the Caribbean Sea will have to be further examined, especially for Fe, Cd, Ni, Zn, Mn whose relatively high

concentrations were detected in the $Si(OH)_4$-enriched surface waters of this study. Additionally, other inputs of trace metals such as atmospheric deposition can also increase surface concentrations, and those inputs can be substantial (Shelley et al., 2012).

4.1.2. Primary production

Primary production rates measured in the oligotrophic surrounding waters were in the lower range of values reported for oligotrophic waters (Laws et al., 2016; Teira et al., 2005). Despite low V_C on D0 and D6 at the DCM, primary production still indicated much higher value on D0 compared to D6 that was associated with higher TChl *a* (Fig. 2a). The decrease of divinyl-chlorophyll *a* concentration, a biomarker of *Prochlorococcus* (Goericke and Repeta, 1992), over the 6 days of observation can account for the decrease of TChl *a*, whereas chlorophyll *a* concentrations did not vary significantly during this period. The *Prochlorococcus* abundance was also lower by two-times on D6 compared to D0 (Fig. 4a). On the contrary, fucoxanthin (diatoms) increased by four-times over the 6 days (Fig. 2a), as well as the diatoms abundance (by three-times; Fig. 3a). In turn, the increase in diatoms abundance was not associated with an increase in primary production. Instead, the observed decrease in primary production can be due to the decrease in *Prochlorococcus* abundance. In tropical and subtropical waters, pico-phytoplankton can indeed contribute to more than 80 % of the primary production (Platt et al., 1983; Goericke and Welschmeyer, 1993). The development of diatoms population likely did not compensate the large decrease in *Prochlorococcus* abundance (from 141,000 to 63,000 cells.mL^{-1}).

4.2. Impact of deep seawater discharge

4.2.1. Temperature effects

The numerical simulation showed that the area impacted in the top-150 m by a temperature difference larger than or equal to 0.3 °C (absolute value) was lower than 1 km^2 (~2-3 % of the considered domain) and was insensitive to the injection depth or to the size of the tested domain (Table 2). The impact of a 0.3 °C temperature variation on the growth of diatoms, notably on *Pseudonitzschia pseudodelicatissima* species that were observed in our study area, is limited to a change in the growth rate of 0.03 d^{-1} (Lundholm et al., 1997). For *Synechococcus*, a 0.3 °C variation of the temperature would also have a limited impact on the growth, with a variation of only 0.02 d^{-1} (Boyd et al., 2013), like for *Emiliania huxleyi* (coccolithophyceae) for which the induced variation of maximum growth rate will be lower than 0.01 d^{-1} (Fielding, 2013). The thermal effect on the phytoplankton assemblage could thus be considered negligible.

4.2.2. Impact on the phytoplankton community

Microcosms enrichment of DCM waters with 10 % of deep seawater led after 6 days to a significant increase ($p < 0.05$) of fucoxanthin (diatoms) and 19'-butanoyloxyfucoxanthin (haptophytes) by 71 % and 77 %, respectively, as compared to the controls. If the 2 % enrichment also showed similar trends, the differences of diagnostic pigments concentrations were not significant. NO_3^- and PO_4^{3-} concentrations induced by 10 % deep-water input on D0 (2.57 ± 0.13 µM and 0.14 ± 0.2 µM, respectively; Giraud et al., 2016) were close to NO_3^- and PO_4^{3-} half-saturation constants of diatoms (1.6 ± 1.9 µM and 0.24 ± 0.29 µM, respectively; Sarthou et al., 2005). The 10 % enrichment could thus support a development of diatoms. On the contrary, NO_3^- and PO_4^{3-} enrichments induced by 2 % addition of deep-water were too low (0.57 ± 0.02 µM and 0.04 ± 0.00 µM, respectively; Giraud et al., 2016) compared to these half-saturation constants to support the diatoms development. Therefore, the diagnostic pigments suggested a significant response proportionally to the amount of added deep seawater.

Prochlorococcus were also more abundant ($p < 0.05$) in 2 % and 10 % treatments as compared to the controls. This lack of further *Prochlorococcus* population increase in 10 % treatments could be attributed to a higher grazing pressure by haptophytes and/or to NO_3^- and PO_4^{3-} too rich conditions (Giraud et al., 2016).

Phytoplankton assemblage widely evolved in surrounding waters, from a predominance of pico-phytoplankton (*Prochlorococcus*) on D0 towards a higher abundance of micro-phytoplankton (diatoms) on D6. In order to assess if the impact on the phytoplankton assemblage due to 10 % deep seawater addition (with a shift towards the diatoms) was in the range of the natural variation observed in the surrounding surface waters, 10 % deep seawater microcosms phytoplankton assemblage was compared to the natural phytoplankton assemblage.

Whereas microcosm controls showed a lower *Prochlorococcus* abundance (Fig. 7a) than surrounding surface waters on D6 ($p < 0.05$), the 10 % microcosms additionally showed, higher fucoxanthin (diatoms) and 19'-butanoyloxyfucoxanthin (haptophytes) by about 142 % and 317 % (Fig. 6), respectively, as compared to natural waters at D6. Furthermore, 10 % enrichments showed a fucoxanthin increase over the 6 days period by 3-times higher than in surrounding waters, whereas controls only showed an increase by 1.5-times higher than in surrounding waters. Therefore, it can be concluded that the 10 % deep seawater enrichment induced higher variations of the phytoplankton assemblage than those observed from D0 to D6 in surrounding surface waters.

445 V_C were higher ($p < 0.05$) both in 2 % and 10 % enrichments on D0 as compared to controls, suggesting a
446 positive response of phytoplankton to the deep seawater addition. Conversely, there was no carbon-uptake
447 rate difference ($p < 0.05$) between controls and enriched waters (with 2 % and 10 % of deep seawater) at D6
448 with the 6 days incubated microcosms, suggesting that the observed community modifications did not change
449 the primary production. Indeed, the phytoplankton community was quite similar in surrounding surface waters
450 on D6 and in 6 days-incubated microcosm controls. Thus, only the initial phytoplankton assemblage and initial
451 primary production in surrounding surface waters would influence the response of the phytoplankton
452 community and its production.

453 At the BEL, after 6 days of incubation, deep seawater addition experiments clearly showed lower effects
454 on the phytoplankton community than at the DCM. Indeed, whereas significant differences ($p < 0.05$) between
455 10 % enrichments and controls were observed in diagnostic pigments concentrations at the DCM, pigments
456 concentrations were too low at the BEL to be quantified. It can be suggested that the lower population and
457 lower carbon uptake could be related to the lowest light availability.

458 Overall, the phytoplankton response was proportional to the amount of added deep seawater. If the
459 phytoplankton assemblage significantly varied over time in the environment, the 10 % deep seawater
460 enrichment showed larger variations (for diatoms and haptophytes) than those observed in the natural
461 environment. The DCM should be more impacted than the BEL by the deep seawater discharge even with a
462 large deep seawater input. On the other hand, the impact on the primary production largely depended on the
463 initial phytoplankton assemblage, which was quite variable over time. The modification of the phytoplankton
464 community to a deep seawater input could also be depending on the initial phytoplankton community. For that,
465 the microcosm experiments did not allow drawing a scenario over the long term of the potential modifications
466 of the primary production and the phytoplankton community associated to the deep seawater discharge by an
467 OTEC.

468 Finally, light microscopy analyses showed a large abundance of dinoflagellates at the DCM (between 9,240
469 and 20,400 cells.mL^{-1} on D6 and D4; Fig. 3 a) which could be mixotrophic or heterotrophic and thus probably
470 exert a grazing pressure on the phytoplankton, particularly on the pico-phytoplankton (Liu et al., 2002).
471 However, in this study, the zooplankton larger than 200 µm and its potential control on the phytoplankton
472 community were not considered and should be examined in future studies.

5. Conclusion

Two complementary approaches were applied to study the potential effects of the deep seawater discharge of the planned OTEC plant on the phytoplankton community in oligotrophic waters off Martinique.

Because the distribution and the development of phytoplankton are directly linked to the surface stratification, it is important to assess the thermal effect of deep seawater by an OTEC plant. Modelling of the deep seawater discharge showed that the thermal structure of the top 150 m of the water column on large and near-OTEC sections should be very slightly impacted for the lowest considered temperature differences $|\Delta T| \geq 0.3$ °C. If World Bank Group prescriptions of not exceeding a higher temperature difference of 3 °C are followed, the environmental perturbations potentially caused by the operation of the OTEC should be considered negligible. The area where the 150 m-depth waters are impacted by the lowest considered temperature differences $|\Delta T| \geq 0.3$ °C would not exceed 1 km^2 in a worst-case scenario.

The phytoplankton community and its production could be impacted by a large deep seawater input. Whereas pico-phytoplankton currently largely dominates the phytoplankton assemblage, a ratio of 10 % of deep seawater in DCM waters could induce a shift toward the diatoms and micro-phytoplankton. The ratio of 2 % of deep seawater in DCM waters only showed significant higher *Prochlorococcus* abundance than controls, but the assemblage and the primary production were not modified by this lower input. The stimulation of *Prochlorococcus* could be due to one or some of the following causes: NO_3^- and/or PO_4^{3-} supply, trace metal supply, lowered pH (higher availability of dissolved inorganic carbon). Since the lower impact on the phytoplankton assemblage was obtained at BEL, this depth can be recommended for the discharge the deep seawater to exploit the OTEC plant.

Although significant, these results would have to be extended to larger temporal scale, and the phytoplankton interactions with higher trophic levels (such as zooplankton) must be studied.

Because no environment standards on the deep seawater discharge effects are available yet, a rigorous monitoring of the phytoplankton community, biogeochemical parameters distribution and of the water column stratification must be established as soon as the OTEC is implemented and during its continuous functioning.

Acknowledgements

This work was supported by France Energies Marines and part of the IMPALA project. We would like to thank the Captains and crew members of the "Pointe d'Enfer", and the scientists in the laboratory at the University of

501 the French West Indies and Guiana at Martinique; Dominique Marie (UPMC, Roscoff, France) and Christophe
502 Lambert (LEMAR, France) for their help with the flow cytometry, and Anne Donval (LEMAR, France) for the
503 pigment analyses.
504
505

References

Agawin, N.S.R., Duarte, C.M., Agustí, S.: Nutrient and temperature control of the contribution of picoplankton to phytoplankton biomass and production. Limnology and Oceanography, 45(8), 1891–1891, 2000.

Aminot, A., and Kérouel, R.: Dosage automatique des nutriments dans les eaux marines : méthodes en flux continu. Ifremer Eds., Méthodes d'analyse en milieu marin, Quae, 2007.

Aure, J., Strand, O., Erga, S.R., Strohmeier, T.: Primary production enhancement by artificial upwelling in a western Norwegian fjord, Marine Ecology Progress Series, 39–470 52, 2007.

Bakun, A.: Global climate change and intensification of coastal ocean upwelling, Science, 247(4939), 198–201, 1990.

Boyd, P. W., Jickells, T., Law, C. S., Blain, S., Boyle, E. A., Buesseler, K. O., et al.: Mesoscale iron enrichment experiments 1993-2005: Synthesis and future directions, Science, 315(5812), 612–617, 2007.

Boyd, P.W., Rynearson, T.A., Armstrong, E.A., Fu, F., Hayashi, K., Hu, Z. et al.: Marine phytoplankton temperature versus growth responses from polar to tropical waters–outcome of a scientific community-wide study, PLoS One, 8(5), e63091, 2013.

Bruland, K. W., Rue, E. L., Smith, G. J.: Iron and macronutrients in California coastal upwelling regimes: Implications for diatom blooms, Limnology and Oceanography, 46, 1661–1674, 2001.

Bruland, K.W.: Controls on trace metals in seawater, The Oceans and Marine Geochemistry, Treatise on Geochemistry, 6, 23-47, 2003.

Brzezinski, M.A.: The Si:C:N ratio of marine diatoms. Interspecific variability and the effect of environmental variables, Journal of Phycology, 21, 347–357, 1985.

Carr, M. E., and Kearns, E. J.: Production regimes in four Eastern Boundary Current systems, Deep Sea Research Part II: Topical Studies in Oceanography, 50(22), 3199–3221, 2003.

Carton, J.A., and Giese, B.S.: A reanalysis of ocean climate using Simple Ocean Data Assimilation (SODA), Monthly Weather Review, 136(8), 2999–3017, 2008.

Casey, J. R., Lomas, M.W., Mandecki, J., Walker, D.E.: Prochlorococcus contributes to new production in the Sargasso Sea deep chlorophyll maximum. Geophysical Research Letters, 34(10), 2007.

Chavez, F.P., Toggweiler, J.R.: Physical estimates of global new production: the upwelling contribution. In: Summerhayes, C.P., Emeis, K.C., Angel, M.V., Smith, R.L., Zeitzschel, B. (Eds.), Upwelling in the Ocean: Modern Processes and Ancient Records. Wiley, 313–320, 1995.

De Baar, H. J., Boyd, P. W., Coale, K. H., Landry, M. R., Tsuda, A., et al.: Synthesis of iron fertilization experiments: from the Iron Age in the age of enlightenment, Journal of Geophysical Research: Oceans (1978–2012), 110(C9), 2005.

Duarte, C.M., Agusti, S., Agawin, N.S.R.: Response of a Mediterranean phytoplankton community to increased nutrient inputs: a mesocosm experiment, Marine Ecology Progress Series, 195, 61–70, 2000.

Dugdale, R.C., and Wilkerson, F.P.: The use of ^{15}N to measure nitrogen uptake in eutrophic oceans; experimental considerations, Limnology and Oceanography, 31(4), 673–689, 1986.

Dulaquais, G., Boye, M., Rijkenberg, M.J.A., Carton, X.J.: Physical and remineralization processes govern the cobalt distribution in the deep western Atlantic Ocean. Biogeosciences, 11(6), 1561–1580, 2014.

Dussart, B.M.: Les différentes catégories de plancton, Hydrobiologia, 26, 72–74, 1966.

Escaravage, V., Prins, T.C., Smaal, A.C., Peeters, J.C.H.: The response of phytoplankton communities to phosphorus input reduction in mesocosm experiments, Journal of Experimental Marine Biology and Ecology, 198, 55–79, 1996.

Fernández, I., Raimbault, P., Garcia, N., Rimmelin, P., Caniaux, G.: An estimation of annual new production and carbon fluxes in the northeast Atlantic Ocean during 2001, Journal of Geophysical Research: Oceans (1978–2012), 110(C7), C07S13, 2005.

Fielding, S.R.: *Emiliania huxleyi* specific growth rate dependence on temperature, Limnol. & Oceanogr, 58(2), 663–666, 2013.

Giraud, M. : Evaluation de l'impact potentiel d'un upwelling artificiel lié au fonctionnement d'une centrale à énergie thermique des mers sur le phytoplancton, Doctorat de l'Université de Bretagne Occidentale, 150 p., 2016.

Giraud, M., Boye, M., Garçon, V., Donval, A., De La Broise, D.: Simulation of an artificial upwelling using immersed in situ phytoplankton microcosms, Journal of Experimental Marine Biology and Ecology, 475, 80–88, 2016.

560 Goericke, R. and Welschmeyer, N.A.: The Marine Prochlorophyte *Prochlorococcus* Contributes Significantly to
561 Phytoplankton Biomass and Primary Production in the Sargasso Sea, Deep Sea Research Part I: Oceanographic
562 Research Papers, 40(11), 2283-2294, 1993.
563 Goericke, R., and Repeta, D.J.: The pigments of *Prochlorococcus marinus*: The presence of divinyl chlorophyll a
564 and b in a marine prochlorophyte. Limnology and Oceanography, 37, 425–433, 1992.
565 Gruber, N.: The marine nitrogen cycle: overview and challenges, Nitrogen in the marine environment, 1–50,
566 2008.
567 Handå, A., McClimans, T.A., Reitan, K.I., Knutsen, Ø., Tangen, K., Olsen, Y.: Artificial upwelling to stimulate
568 growth of non-toxic algae in a habitat for mussel farming, Aquaculture Research, 45, 1798–1809, 2014.
569 Harrison, W.G., Harris, L.R., Irwin, B.D.: The kinetics of nitrogen utilization in the oceanic mixed layer: Nitrate
570 and ammonium interactions at nanomolar concentrations, Limnology and Oceanography, 41(1), 16–32, 1996.
571 Hasle, G.R.: The inverted microscope method, In: Sournia, A. (Ed.), Phytoplankton Manual. UNESCO, Paris,
572 1988.
573 Hillebrand, H., Durselen, C.D., Kirchttel, D., Pollingher, U., Zohary, T.: Biovolume calculation for pelagic and
574 benthic microalgae, Journal of Phycology, 35, 403–424, 1999.
575 Hooker, S.B., Clementson, L., Thomas, C.S., Schlüter, L., Allerup, M., Ras, J., Claustre, H., et al.: NASA
576 Tech. Memo. 2012-217503, NASA Goddard Space Flight Center, Greenbelt, Maryland, 2012.
577 Hutchins, D.A., Hare, C.E., Weaver, R.S., Zhang, Y., Firme, G.F., DiTullio, G.R., Alm, M.B., Riseman, S.F.,
578 Maucher, J.M., Geesey, M.E., Trick, C.G., Smith, G.J., Rue, E.L., Conn, J., Bruland, K.W.: Phytoplankton
579 iron limitation in the Humboldt current and Peru upwelling, Limnology and Oceanography, 47, 997–1011,
580 2002.
581 International Finance Corporation (IFC): World Bank Group, Environmental, Health, and Safety Guidelines for
582 Liquefied Natural Gas (LNG) Facilities, 2007.
583 Kagaya, S., Maeba, E., Inoue, Y., Kamichatani, W., et al.: A solid phase extraction using a chelate resin
584 immobilizing carboxymethylated pentaethylenehexamine for separation and preconcentration of trace elements
585 in water samples, Talanta, 79(2), 146–152, 2009.
586 Kress, N., Thingstad, T.F., Pitta, P., Psarra, S., Tanaka, T., Zohary, T., Groom, S., Herut, B., Mantoura, R.F.C.,
587 Polychronaki, T., Rassoulzadegan, F., Spyres G.: Effect of P and N addition to oligotrophic Eastern

588 Mediterranean waters influenced by near-shore waters: a microcosm experiment, Deep Sea Research Part II:
589 Topical Studies in Oceanography, 52, 3054–3073, 2005.
590 Laws, E.A., Bidigare, R.R., Karl, D.M.: Enigmatic relationship between chlorophyll a concentrations and
591 photosynthetic rates at Station ALOHA, Heliyon, 2, e00156, 2016.
592 Liu, H., Suzuki, K., Saino, T.: Phytoplankton growth and microzooplankton grazing in the subarctic Pacific Ocean
593 and the Bering Sea during summer 1999, Deep Sea Research Part I: Oceanographic Research Papers, 49(2),
594 363–375, 2002.
595 Lundholm, N., Skov, J., Pocklington, R., Moestrup, Ø.: Studies on the marine planktonic diatom *Pseudo-*
596 *nitzschia*. 2. Autecology of *P. pseudodelicatissima* based on isolates from Danish coastal waters, Phycologia,
597 36(5), 381–388, 1997.
598 Marie, D., Partensky, F., Vaulot, D., Brussaard, C.: Enumeration of phytoplankton, bacteria, and viruses in marine
599 samples, Current protocols in cytometry, 1–11, 1999.
600 Mawji, E., Schlitzer, R., et al.: The GEOTRACES intermediate data product 2014, Marine Chemistry, 177(1),
601 1-8, 2015, doi 10.1016/j.marchem.2015.04.005. `
602 Milne, A., Landing, W., Bizimis, M., Morton, P.: Determination of Mn, Fe, Co, Ni, Cu, Zn, Cd and Pb in seawater
603 using high resolution magnetic sector inductively coupled mass spectrometry (HR-ICP-MS). Analytica Chimica
604 Acta, 665(2), 200–207, 2010.
605 National Oceanic and Atmospheric Administration (NOAA): Ocean thermal energy conversion final
606 environmental impact statement. Office of Ocean Minerals and Energy, Charleston, SC, 1981.
607 National Oceanic and Atmospheric Administration (NOAA): Ocean thermal energy conversion: Assessing
608 potential physical, chemical, and biological impacts and risks. University of New Hampshire, Durham, NH, 2010.
609 Nozaki, Y.: A fresh look at element distribution in the North Pacific Ocean, Eos Transaction, 78(21), 221, 1997.
610 Orr, J.C., Fabry, V.J., Aumont, O., Bopp, L., Doney, S.C., Feely, R.A., Gnanadesikan, A., Gruber, N., Ishida, A., Joos, F., Key,
611 R.M., Lindsay, K., Maier-Reimer, E., Matear, R., Monfray, P., Mouchet, A., Najjar, R.G., Plattner, G.K., Rodgers, K.B., Sabine,
612 C.L., Sarmiento, J.L., Schlitzer, R., Slater, R.D., Totterdell, I.J., Weirig, M.F., Yamanaka, Y., Yool, A.: Anthropogenic ocean
613 acidification over the twenty-first century and its impact on calcifying organisms, Nature, 437(7059), 681–686,
614 2005.
615 Partensky, F., Hess, W.R., Vaulot, D.: *Prochlorococcus*, a marine photosynthetic prokaryote of global
616 significance, Microbiology and Molecular Biology Reviews, 63 (1), 106–127, 1999.

617 Pauly, D., and Christensen, V.: Primary production required to sustain global fisheries, Nature, 374(6519), 255–
618 257, 1995.
619 Platt, T., Rao, D. S., Irwin, B.: Photosynthesis of picoplankton in the oligotrophic ocean, Nature, 301, 702–704,
620 1983.
621 Rocheleau, G., Hamrick, J., Church, M.: Modeling the Physical and Biochemical Influence of Ocean Thermal
622 Energy Conversion Plant Discharges into their Adjacent Waters, Final Technical Report, U.S. Department of
623 Energy Award N° DE-EE0003638, Makai Ocean Engineering, Inc., Kailua, Hawaii, 2012.
624 Sarthou, G., Timmermans, K.R., Blain, S., Tréguer, P.: Growth physiology and fate of diatoms in the ocean: a
625 review, Journal of Sea Research, 53(1), 25–42, 2005.
626 Shchepetkin, A.F., and McWilliams, J.C.: Correction and commentary for "Ocean forecasting in terrain-following
627 coordinates: Formulation and skill assessment of the regional ocean modeling system" by Haidvogel et al., J.
628 Comp. Phys., 227, 3595–3624, Journal of Computational Physics, 228(24), 8985–9000, 2009.
629 Shchepetkin, A.F., and McWilliams, J.C.: The regional oceanic modeling system (ROMS): a split-explicit, free-
630 surface, topography-following-coordinate oceanic model, Ocean Modelling, 9(4), 347–404, 2005.
631 Shelley, R. U., et al.: Controls on dissolved cobalt in surface waters of the Sargasso Sea: Comparisons with iron
632 and aluminum, Global Biogeochem. Cycles, 26(2), GB2020, doi:10.1029/2011GB004155, 2012.
633 Slawyk, G., Collos, Y., Auclair, J.C.: The use of the ^{13}C and ^{15}N isotopes for the simultaneous measurement of
634 carbon and nitrogen turnover rates in marine phytoplankton, Limnology and Oceanography, 22, 925–932, 1977.
635 Taguchi, S., Jones, D., Hirata, J.A., Laws, E.A.: Potential effect of ocean thermal energy conversion (OTEC)
636 mixed water on natural phytoplankton assemblages in Hawaiian waters. Bulletin of Plankton Society of
637 Japan, 34(2), 125–142, 1987.
638 Teira, E., Mouriño, B., Marañón, E., Pérez, V., Pazó, M.J., Serret P, de Armas, D., Escánez, J., Woodward, E.M.S.,
639 Fernández, E.: Variability of chlorophyll and primary production in the Eastern North Atlantic Subtropical Gyre:
640 potential factors affecting phytoplankton activity. Deep-Sea Research I, 52, 569-288, 2005.
641 Thomas, C.R.: Identifying Marine Phytoplankton. Academic Press, Inc. San Diego, California, 1996.
642 Tovar-Sanchez, A., and Sañudo-Wilhelmy, S.A.: Influence of the Amazon River on dissolved and intra-cellular
643 metal concentrations in *Trichodesmium* colonies along the western boundary of the sub-tropical North Atlantic
644 Ocean, Biogeosciences, 8, 217–225, 2011.

645 Uitz, J., Claustre, H., Gentili, B., Stramski, D.: Phytoplankton class-specific primary production in the world's
646 oceans: seasonal and interannual variability from satellite observations, Global Biogeochemical Cycles, 24(3),
647 2010.
648 Van Oostende, N., Dunne, J. P., Fawcett, S. E., Ward, B. B.: Phytoplankton succession explains size-partitioning
649 of new production following upwelling-induced blooms, Journal of Marine Systems, 148, 14–25, 2015.
650 WoRMS Editorial Board: World Register of Marine Species. Available from http://www.marinespecies.org at VLIZ.
651 Accessed 2019-06-21. doi:10.14284/170), 2019.
652

Tables

Table 1- Comparison of analyses of SAFe (Sampling and Analysis of iron) S and D2 reference samples (http://www.geotraces.org/science/intercalibration) between ID-ICPMS values (this study) and the consensus values. Our mean reagent blanks (based on all blank determinations) for dissolved Cd, Pb, Fe, Ni, Cu, Zn, Mn and Co, and detection limits of ID-ICPMS estimated as three times the standard deviation of the mean reagent blanks are also shown.

	Cd (pM)	Pb (pM)	Fe (nM)	Ni (nM)	Cu (nM)	Zn (nM)	Mn (nM)	Co (pM)
SAFe D2								
This study	948.83 ± 65.95	28.86 ± 4.44	0.898 ± 0.098	8.60 ± 0.36	2.15 ± 0.16	7.29 ± 0.27	0.40 ± 0.05	40.12 ± 3.88
Consensus values	986.00 ± 23.00	27.70 ± 1.50	0.933 ± 0.023	8.63 ± 0.25	2.28 ± 0.15	7.43 ± 0.25	0.35 ± 0.05	45.70 ± 2.90
n=	20	20	18	19	22	13	23	23
SAFe S								
This study	7.24 ± 1.57	48.42 ± 6.08	0.087 ± 0.025	2.56 ± 0.55	0.55 ± 0.06	0.07 ± 0.06	0.75 ± 0.05	2.85 ± 0.81
Consensus values	1.10 ± 0.30	48.00 ± 2.20	0.093 ± 0.008	2.28 ± 0.09	0.52 ± 0.05	0.07 ± 0.01	0.79 ± 0.06	4.80 ± 1.20
n=	25	27	15	25	30	10	27	28
Detection Limit	0.996	0.613	0.032	0.096	0.011	0.129	0.001	0.07
Blanks	0.716	1.809	0.061	0.040	0.019	0.129	0.003	0.32

Table 2- Area (km^2) (average and root mean square) impacted in the top-150 m by a temperature difference $|\Delta T| \geq 0.3$ °C on two vertical sections centered on the OTEC, considering eight depths of deep seawater discharge (45, 80, 110, 140, 170, 250, 350, 500 m) (Giraud, 2016).

	Annual mean		June	
Depth of deep water discharge	Large domain	Near-OTEC domain	Large domain	Near-OTEC domain
45 m	0.4 ± 0.4	0.0 ± 0.1	0.0	0.0
80 m	0.6 ± 0.7	0.1 ± 0.1	0.4	0.0
110 m	0.6 ± 0.5	0.0 ± 0.1	0.9	0.0
140 m	0.4 ± 0.5	0.1 ± 0.1	0.1	0.0
170 m	0.5 ± 0.8	0.0 ± 0.1	0.5	0.0
250 m	0.5 ± 0.7	0.1 ± 0.1	0.1	0.0
350 m	0.5 ± 0.5	0.1 ± 0.1	0.0	0.0
500 m	0.5 ± 0.5	0.1 ± 0.1	0.3	0.0

Table 3- Nitrate, silicate, phosphate and nitrite concentrations on June 16th 2014 (D4) at the deep chlorophyll maximum (DCM), at the bottom of the euphotic layer (BEL), and at the deep seawater pumping depth. Concentrations were measured at the OTEC site (0 % addition of deep waters) and calculated for 2 % and 10 % deep seawater additions.

Depth (m)	Deep seawater ratio	$[NO_3^-]$ (µM)	$[Si(OH)_4]$ (µM)	$[PO_4^{3-}]$ (µM)	$[NO_2^-]$ (µM)
DCM	0 %	< 0.02	2.39	< 0.02	0.02
	2 %	0.54	2.88	0.04	0.02
	10 %	2.71	4.82	0.19	0.02
BEL	0 %	< 0.02	1.46	< 0.02	0.32
	2 %	0.54	1.96	0.04	0.32
	10 %	2.71	3.98	0.19	0.29
1100	100 %	27.11	26.69	1.87	<0.02

671 **Table 4-** Concentrations of dissolved trace metals (in nM): Mn, Fe, Cd, Zn, Co, Ni, Cu, Pb measured on June
672 16th 2014 (D4) at the OTEC site at the DCM, BEL and 1100 m (0 % addition of deep waters), and their calculated
673 concentrations in the mixtures with 2 % and 10 % addition of deep water.

Depth (m)	Deep seawater ratio	Mn (nM)	Fe (nM)	Cd (nM)	Zn (nM)	Co (nM)	Ni (nM)	Cu (nM)	Pb (nM)
DCM	0 %	2.97 ± 0.17	1.08 ± 0.03	0.03 ± 0.01	1.54 ± 0.04	0.05 ± 0.00	2.22 ± 0.10	1.70 ± 0.18	0.03 ± 0.00
	2 %	2.92	1.08	0.04	1.56	0.05	2.29	1.70	0.03
	10 %	2.71	1.09	0.07	1.63	0.05	2.60	1.71	0.03
BEL	0 %	1.65 ± 0.04	0.68 ± 0.03	0.03 ± 0.00	0.65 ± 0.03	0.03 ± 0.00	2.26 ± 0.17	1.14 ± 0.10	0.03 ± 0.00
	2 %	1.63	0.69	0.04	0.68	0.03	2.34	1.15	0.03
	10 %	1.52	0.73	0.08	0.82	0.03	2.64	1.21	0.03
1100	100 %	0.34 ± 0.02	1.22 ± 0.05	0.45 ± 0.01	2.39 ± 0.07	0.06 ± 0.00	6.00 ± 0.13	1.80 ± 0.08	0.02 ± 0.00

674

675 **Table 5-** Definition of the diagnostic pigments used as phytoplankton biomarkers (taxonomic significance) and
676 associated phytoplankton size class (Uitz et al., 2010).

677

Diagnostic Pigments	Abbreviations	Taxonomic Significance	Phytoplankton Size Class
Fucoxanthin	Fuco	Diatoms	microplankton
Peridinin	Perid	Dinoflagellates	microplankton
19'-hexanoyloxyfucoxanthin	Hex-fuco	Haptophytes	nanoplankton
19'-butanoyloxyfucoxanthin	But-fuco	Pelagophytes and Haptophytes	nanoplankton
Alloxanthin	Allo	Cryptophytes	nanoplankton
chlorophyll *b* + divinyl chlorophyll *b*	TChlb	Cyanobacteria, Prochlorophytes	picoplankton
Zeaxanthin	Zea	Chlorophytes, Prochlorophytes	picoplankton

678

679

680

Figure captions

Figure 1- Bathymetry of the parent and child (grey rectangle) domains interpolated from the GINA data base with a zoom on the near domain (black rectangle); the oblique white and black lines represent the large and small sections, respectively, used for numerical simulations.

Figure 2- Pigment concentrations (from HPLC analysis) at the OTEC site at the DCM (a) and at the BEL (b), on June 12th (D0), 16th (D4), 18th (D6) 2014 (bars represent the standard deviation).

Figure 3- Abundance and biovolume of micro- and part of nano-phytoplankton at the OTEC site on June 12th (D0), 16th (D4), 18th (D6) 2014, at the DCM (a and c, respectively) and at the BEL (b and d, respectively) (bars represent the standard deviation).

Figure 4- Abundance of pico-phytoplankton at the DCM (a) and at the BEL (b), on June 12th (D0), 16th (D4), 18th (D6) 2014 (bars represent the standard deviation).

Figure 5- Specific carbon uptake rate (µmol.(µg Chl *a*)$^{-1}$.h^{-1}) at the DCM (a) and BEL (b) depths, on June 12th (D0), and 18th (D6), and in 6 days incubated microcosms (D6), for the three mixing conditions (0 %, 2 % and 10 % of deep seawater additions) (for surrounding waters bars represent the standard deviation for 2 replicates).

Figure 6- Diagnostic pigment concentrations in surrounding surface waters on D0 and D6, and in controls and deep water-enriched (2 % and 10 %) microcosms after 6 days of incubation at the DCM (bars represent the standard deviation). Similar letters (a, b or c) attributed to 2 or more treatments indicate no significant differences ($p < 0.05$) between these treatments.

Figure 7- Abundance of picophytoplankton in surrounding surface waters on days 0 and 6, and in controls and deep water-enriched (2 % and 10 %) microcosms after 6 days of incubation at 45 m depth (a) and 80 m depth (b) (bars represent the standard deviation). Similar letters (a, b or c) attributed to 2 or more treatments indicate no significant differences ($p < 0.05$) between these treatments.

709 **Figure 1**

710

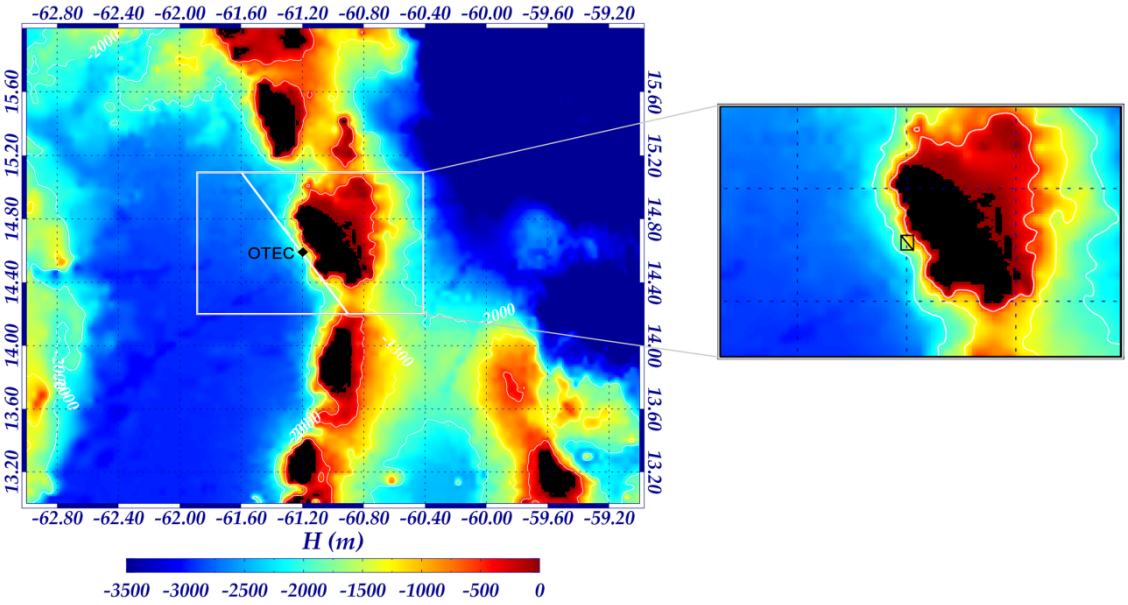

711

712

713

714

715

716

717

718

719

720

721

722

723

724

725

726 **Figure 2**

727

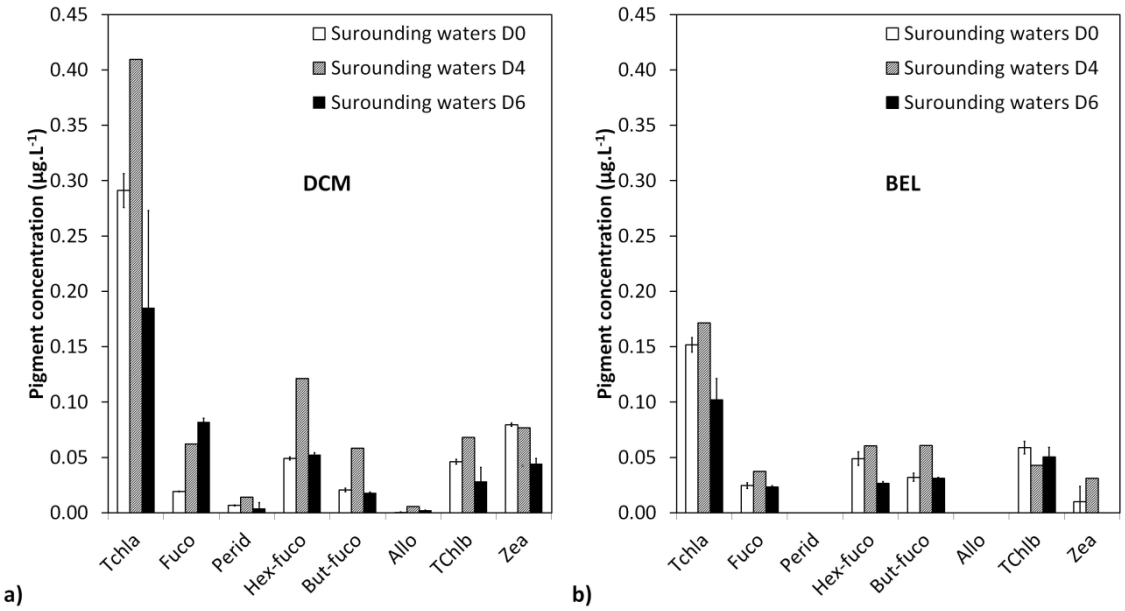

728

729

730

731

732 **Figure 3**

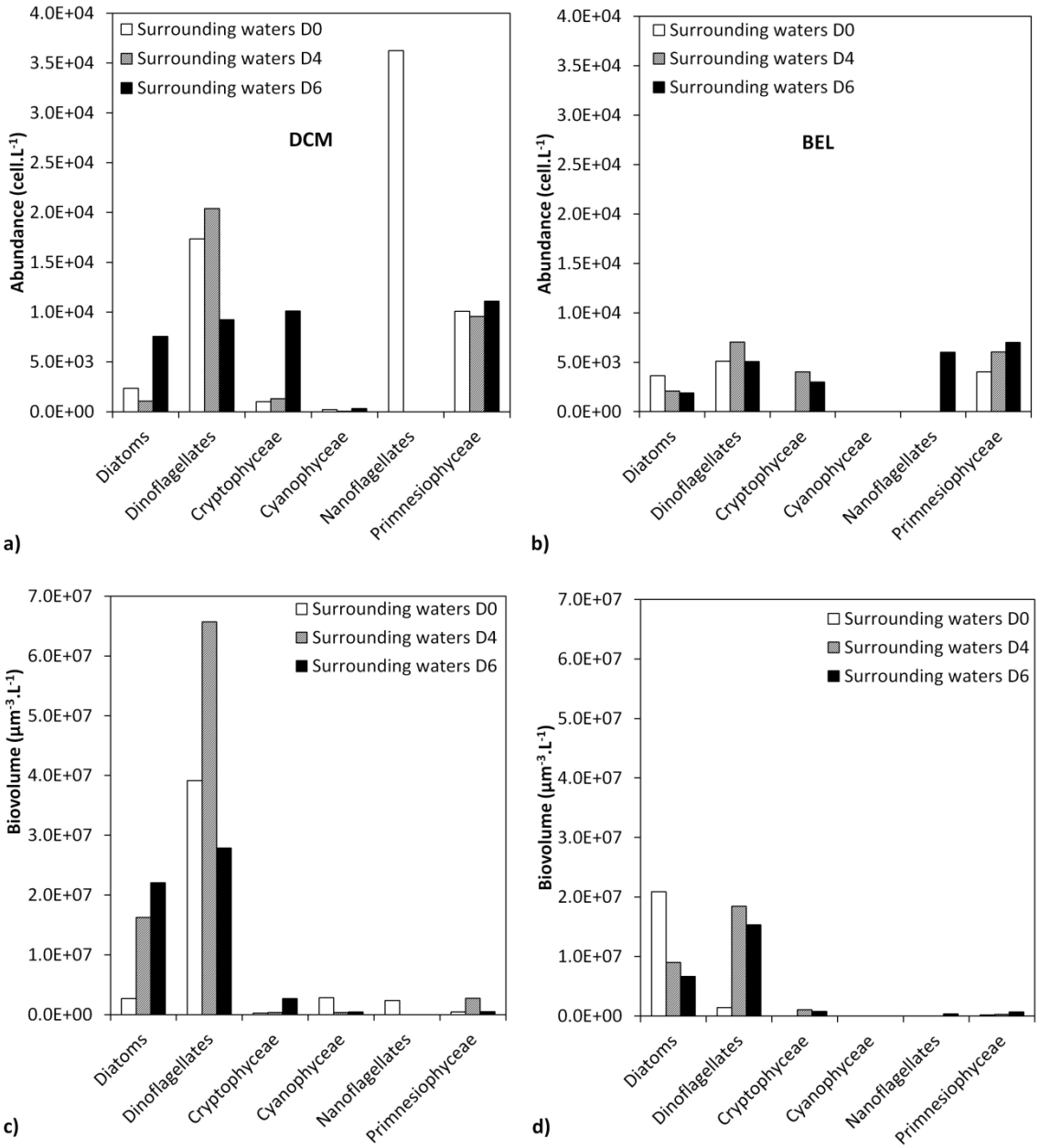

733

734

735

736

737

738

739

740 **Figure 4**

741

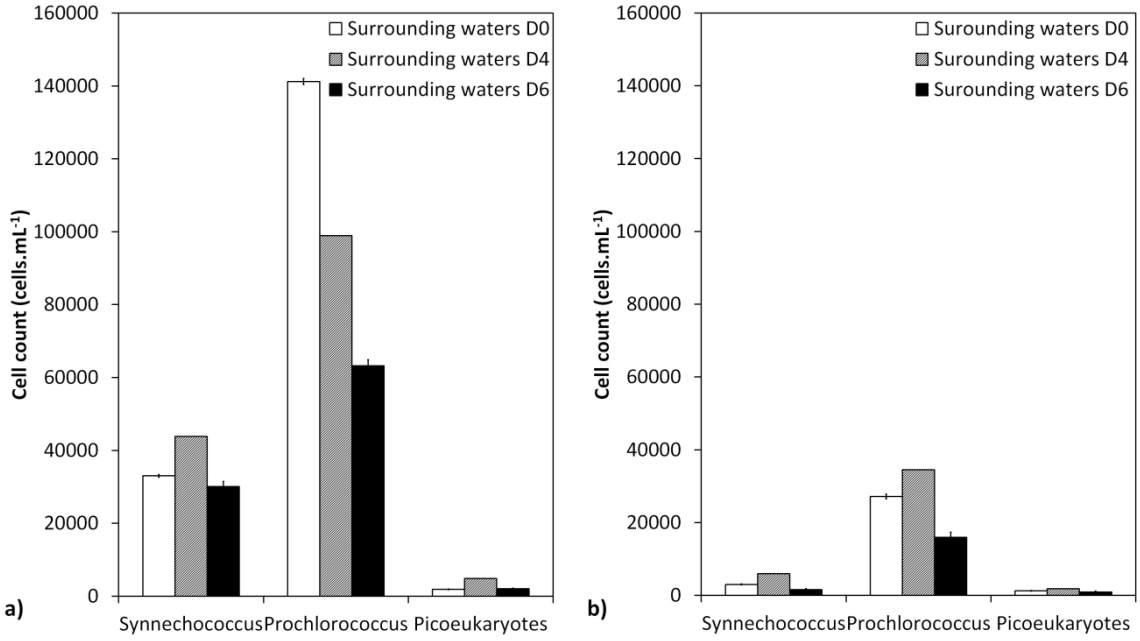

742

743

744

745 **Figure 5**

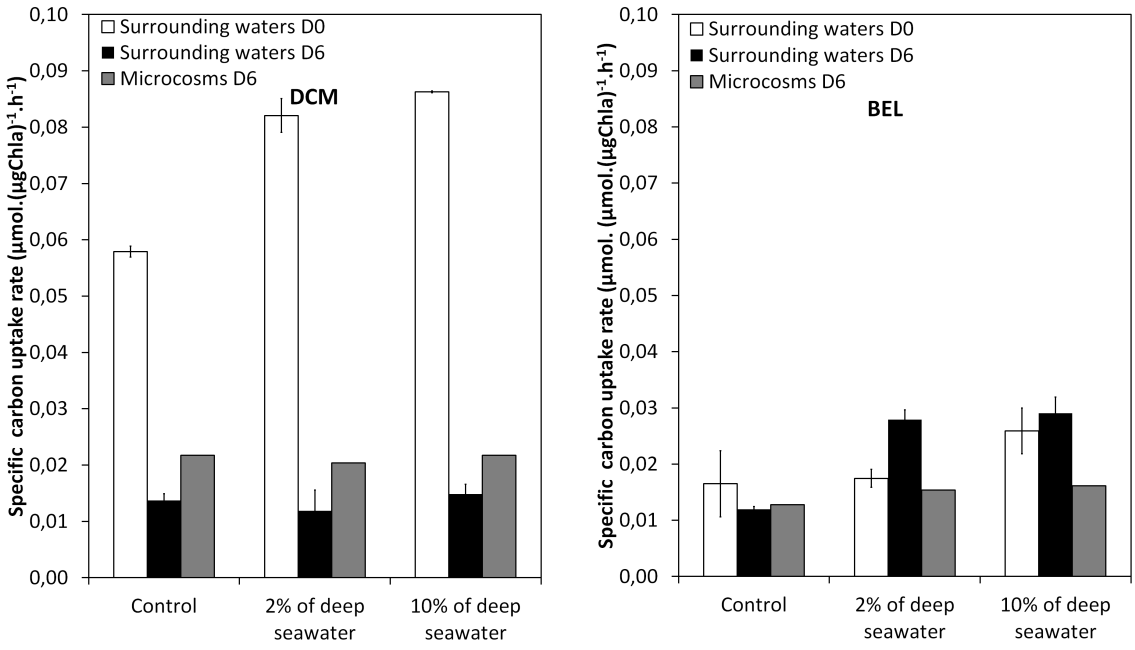

746

747

748

749 **Figure 6**

750

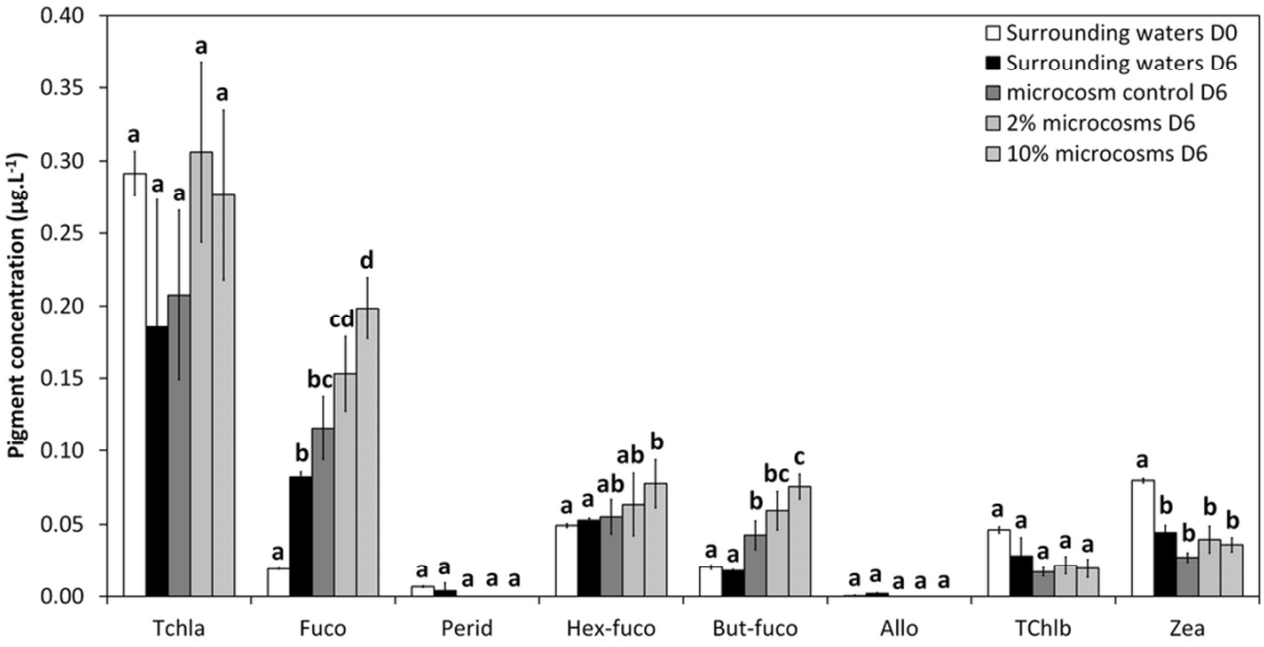

751

752

753

754 **Figure 7**

755

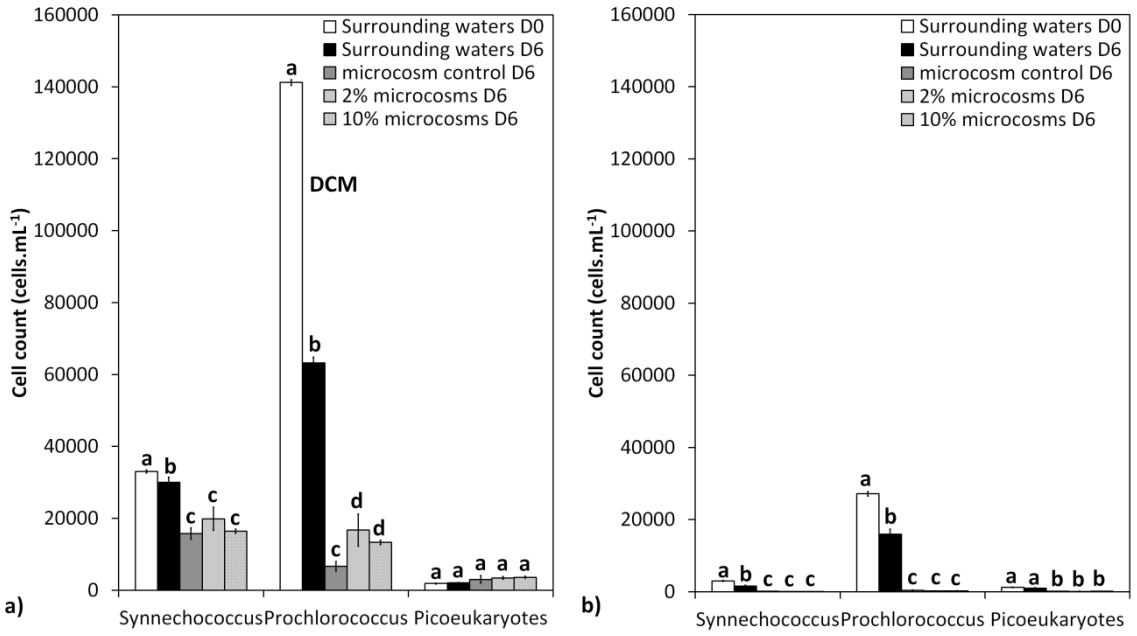

756

757

758